BEAT-TO-BEAT P AND T WAVE DELINEATION IN ECG SIGNALS USING A MARGINALIZED PARTICLE FILTER

Chao Lin[1], *Audrey Giremus*[2], *Corinne Mailhes*[1], *and Jean-Yves Tourneret*[1]

[1]University of Toulouse, IRIT/ENSEEIHT/TéSA, 2 rue Charles Camichel, BP 7122, 31071 Toulouse cedex 7, France
[2]University of Bordeaux, IMS-LAPS-UMR 5218, Talence, France
chao.lin@tesa.prd.fr, audrey.giremus@ims-bordeaux.fr, {jean-yves.tourneret,corinne.mailhes}@enseeiht.fr

ABSTRACT

The delineation of P and T waves is important for the interpretation of ECG signals. In this work, we propose a sequential Bayesian detection-estimation algorithm for simultaneous P and T wave detection, delineation, and waveform estimation on a beat-to-beat basis. Our method is based on a dynamic model which exploits the sequential nature of the ECG by introducing a random walk model to the waveforms. The core of the method is a marginalized particle filter that efficiently resolves the unknown parameters of the dynamic model. The proposed algorithm is evaluated on the annotated QT database and compared with state-of-the-art methods. Its on-line characteristic is ideally suited for real-time ECG monitoring and arrhythmia analysis.

Index Terms— ECG, P and T wave delineation, sequential Monte Carlo methods, particle filtering

1. INTRODUCTION

Electrocardiograms (ECGs) are characterized by a recurrent wave sequence: P wave, QRS complex and T wave[1]. In ECGs, most of the clinically useful information can be found in the intervals, amplitudes, or wave morphology. Therefore, the development of efficient and robust methods for automatic ECG delineation (determination of peaks and limits of the individual waves) and waveform estimation has become a very interesting challenge for biomedical engineers. Among the ECG waves, the QRS complex is relatively easy to detect because of its high and peaky amplitude and is thus generally used as a reference within the cardiac cycle. Concerning P and T wave detection and delineation, most existing methods perform QRS detection first. They then define temporal search intervals before and after the detected QRS location to search for the P and T waves using adaptive filtering [1], low-pass differentiation [2] or the wavelet transform (WT) [3]. Delineation can also be based on the concept of fitting a realistic model to the ECG and extracting parameters from the model to determine waveform onsets and offsets. Particular attention has been devoted to Gaussian mixture models whose parameters can be estimated with extended Kalman filters (EKFs) [4]. Because of the low slope and magnitude of the P and T waves, as well as the presence of noise, interference, and baseline fluctuation, P and T wave delineation remains a complicated task. Furthermore, in addition to the determination of wave peaks and limits, the shapes of P and T waves have also been proved to contain important information about many kinds of diseases [5].

A Bayesian model was recently introduced in [6] for simultaneous P and T wave delineation and waveform estimation. This model takes into account prior distributions for the unknown parameters (wave locations and amplitudes as well as waveform coefficients). These prior distributions are combined with the likelihood of the observed data to obtain the posterior distribution of the unknown parameters. Several Gibbs-type samplers have been proposed to alleviate the computational complexity of this posterior distribution and to estimate the model parameters [6, 7]. However, the Bayesian model introduced in [6] relies on a non-overlapped multiple-beat processing window to estimate the waveforms. More precisely, the waveforms of all P and T waves within a multiple-beat processing window are assumed to be equal, whereas their amplitudes and locations are allowed to vary from one beat to another. Due to the pseudo-cyclostationary nature of the ECG signal, the P and T waveforms in a given beat are usually similar *but not exactly equal* to those of the adjacent beats. Therefore, the performance of P and T wave delineation can be expected to improve if the waveforms are estimated in a *beat-to-beat* manner that allows for temporal variations of waveform morphology across the beats. Moreover, it is typically crucial to process data on-line, both from the point of view of storage costs as well as for rapid adaptation to changing signal characteristics.

In this paper, we propose a dynamic model and an associated particle filter (PF) to solve simultaneously P and T wave delineation and waveform estimation in a beat-to-beat basis. The proposed dynamic model is similar to the Bayesian models introduced in [6, 7]. However, it adapts to the morphology variations across the ECG beats by assigning a random walk model to the waveform coefficients. Following the sequential Monte Carlo (SMC) principle [8], PFs are introduced to estimate the unknown parameters of the proposed model. The key idea is to represent the required posterior density by a set of random samples with associated weights and to compute parameter estimates from these samples and weights. Despite the simplicity of the PF principle, its main drawback is its computational complexity especially for large state dimension. This computational complexity can be reduced for nonlinear dynamic models containing a subset of parameters which are linear and Gaussian, conditional upon the other parameters. In this case, the linear parameters can be optimally estimated through standard linear Gaussian filtering. This technique is often referred to as Rao-Blackwellization [9] or marginalization [10]. In our case, the state equations are linear with respect to a subset of the unknown parameters. Thus we propose to use a marginalized particle filter (MPF) that dismisses the states appearing linearly in the dynamics, generate particles in the space of the remaining states and run one Kalman filter for each of these particles to estimate the "linear" parameters. The proposed approach is evaluated on the annotated QT database [11]. A comparison with the window-based Bayesian method in [6] and other classical methods shows that the proposed sequential model and process-

[1]http://en.wikipedia.org/wiki/File:SinusRhythmLabels.svg

ing improve the accuracy of estimating the locations, amplitudes, and shapes of the P and T waves.

The paper is organized as follows. Section 2 describes the proposed dynamic model for the non-QRS signal components. Section 3 studies the associated MPF. Simulation results using the QT database and a comparison with other classical methods are presented in Section 4. Finally, some conclusions are provided in Section 5.

2. DYNAMIC MODEL FOR A NON-QRS INTERVAL

Non-QRS intervals in an ECG signal are located between a QRS end and the subsequent QRS onset. These intervals potentially contain P and T waves. In this paper, we assume that the locations of the non-QRS intervals are provided by a preliminary QRS detection step using the Pan-Tompkins algorithm [12]. The baseline wandering is removed by a median filtering technique as suggested in [13].

2.1. Signal model

As shown in Fig. 1, the non-QRS interval $\mathcal{J}_n$ associated with the nth heartbeat consists of two complementary subintervals: a T search interval $\mathcal{J}_{\mathrm{T},n}$, which may contain a T wave, and a P search interval $\mathcal{J}_{\mathrm{P},n}$, which may contain a P wave. The lengths of the intervals $\mathcal{J}_n$, $\mathcal{J}_{\mathrm{T},n}$, and $\mathcal{J}_{\mathrm{P},n}$ will be denoted by N_n, $N_{\mathrm{T},n}$, and $N_{\mathrm{P},n}$, respectively. Note that $N_{\mathrm{T},n} + N_{\mathrm{P},n} = N_n$. The interval lengths $N_{\mathrm{T},n}$ and $N_{\mathrm{P},n}$ can be determined by a cardiologist or simply fixed as given percentages of N_n. In this paper, we choose $N_{\mathrm{T},n} = N_{\mathrm{P},n} = N_n/2$. Our goal is to estimate the locations and shapes (waveforms) of the T and P waves within their respective search intervals $\mathcal{J}_{\mathrm{T},n}$ and $\mathcal{J}_{\mathrm{P},n}$.

Similar to the blind deconvolution problem in [6], the signal $y_{n,k}$ in the nth T wave interval $\mathcal{J}_{\mathrm{T},n}$ can be modeled by the convolution of an unknown binary "indicator sequence" $\boldsymbol{b}_{\mathrm{T},n} = (b_{\mathrm{T},n,1} \cdots b_{\mathrm{T},n,N_{\mathrm{T},n}})^T$ indicating the wave locations ($b_{\mathrm{T},n,i} = 1$ if there is a wave at location i, $b_{\mathrm{T},n,i} = 0$ otherwise) with an unknown T waveform $\boldsymbol{h}_{\mathrm{T},n} = (h_{\mathrm{T},n,-L} \cdots h_{\mathrm{T},n,L})^T$ such that

$$y_{n,k} = \sum_{j=1}^{N_{\mathrm{T},n}} h_{\mathrm{T},n,k-j}\, b_{\mathrm{T},n,j} + w_{n,k}\,, \quad k \in \mathcal{J}_{\mathrm{T},n} \tag{1}$$

where $w_{n,k}$ is a white Gaussian noise with variance $\sigma^2_{w,n}$ and $h_{\mathrm{T},n,k} = 0$ for $k \notin \{-L, \ldots, L\}$. The waveform length $2L+1$ is chosen as a fixed percentage of N_n that is large enough to accommodate the actual supports of the T wave (e.g., $N_n/3$ in this work). The signal model ensures that the position of a nonzero detected indicator (such that $\hat{b}_{\mathrm{T},n,k} = 1$) directly indicates the center $k=0$ of the waveform support interval $\{-L, \ldots, L\}$. Note that since there is at most one T wave in each T wave interval, there will be at most one nonzero entry of $\boldsymbol{b}_{\mathrm{T},n}$ which corresponds to the T wave location.

Similarly, the P wave within the P wave interval is modeled by the convolution of $\boldsymbol{h}_{\mathrm{P},n} = (h_{\mathrm{P},n,-L} \cdots h_{\mathrm{P},n,L})^T$ with $\boldsymbol{b}_{\mathrm{P},n} = (b_{\mathrm{P},n,1} \cdots b_{\mathrm{P},n,N_{\mathrm{P},n}})^T$. The P interval signal component $y_{n,k}$ can then be written as

$$y_{n,k} = \sum_{j=1}^{N_{\mathrm{P},n}} h_{\mathrm{P},n,k-j}\, b_{\mathrm{P},n,j} + w_{n,k}\,, \quad k \in \mathcal{J}_{\mathrm{P},n} \tag{2}$$

with $h_{\mathrm{P},n,k} = 0$ for $k \notin \{-L, \ldots, L\}$.

Following [7], we represent the T and P waveforms by a basis expansion using discrete-time versions of Hermite functions. Thus, the waveform vectors can be written as

$$\boldsymbol{h}_{\mathrm{T},n} = \boldsymbol{H}\boldsymbol{\alpha}_{\mathrm{T},n}\,, \quad \boldsymbol{h}_{\mathrm{P},n} = \boldsymbol{H}\boldsymbol{\alpha}_{\mathrm{P},n} \tag{3}$$

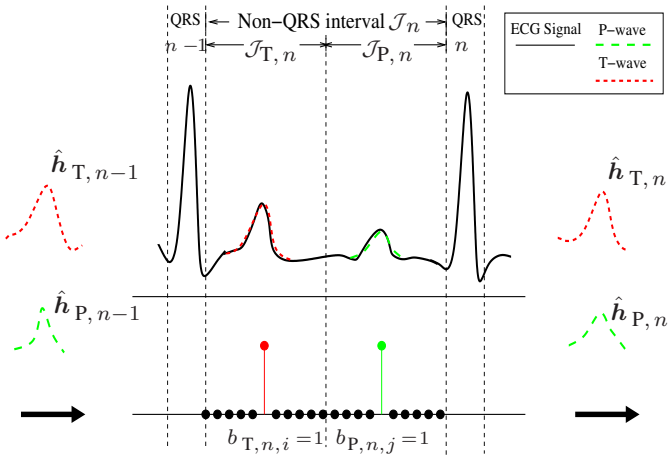

Fig. 1. Signal model within a non-QRS interval.

where $\boldsymbol{H}$ is a $(2L+1) \times G$ matrix whose columns are the first G Hermite functions (with $G \leq 2L+1$), suitably sampled and truncated to length $2L+1$, $\boldsymbol{\alpha}_{\mathrm{T},n}$ and $\boldsymbol{\alpha}_{\mathrm{P},n}$ are unknown coefficient vectors of length G. By using these expansions, the number of unknown parameters can be reduced from $2L+1$ to G for each waveform (e.g., we have chosen $G = 20$ and $2L+1$ is around 83 for ECGs with heart rate around 60 beats per minute and sampled at 250Hz).

Using (3), we obtain the following vector representation of the T wave interval in (1)

$$\boldsymbol{y}_{\mathrm{T},n} = \boldsymbol{B}_{\mathrm{T},n}\boldsymbol{H}\boldsymbol{\alpha}_{\mathrm{T},n} + \boldsymbol{w}_n \tag{4}$$

where $\boldsymbol{y}_{\mathrm{T},n} = (y_{n,1} \cdots y_{n,N_{\mathrm{T},n}})^T$, $\boldsymbol{B}_{\mathrm{T},n}$ is the $(N_{\mathrm{T},n}) \times (2L+1)$ Toeplitz matrix with first row $(b_{n,L+1} \cdots b_{n,1}\ 0 \cdots 0)$ and first column $(b_{n,L+1} \cdots b_{n,N_{\mathrm{T},n}}\ 0 \cdots 0)^T$ and $\boldsymbol{w}_n = (w_{n,1} \cdots w_{n,N_{\mathrm{T},n}})^T$ is a Gaussian vector with covariance matrix $\sigma^2_w \boldsymbol{I}_{N_{\mathrm{T},n} \times N_{\mathrm{T},n}}$. Note that similar vector representation can be obtained for the P wave interval $\boldsymbol{y}_{\mathrm{P},n} = (y_{n,N_{\mathrm{T},n}+1} \cdots y_{n,N_n})^T$.

2.2. Prior distributions and dynamic model

This section describes the prior distributions and the dynamic model assigned to the unknown parameters. The proposed algorithm successively processes the T and P wave intervals within the same non-QRS component in a *fully analogous way*. Note that only the T wave dynamic model is presented in the following and the subscript indicating T wave is omitted for notation convenience.

Due to the parametrization (4), the state parameter vector for the nth T wave interval (time step n) is given by

$$\boldsymbol{x}_n = \left(\boldsymbol{b}_n^T,\ \boldsymbol{\alpha}_n^T\right)^T. \tag{5}$$

Concerning the indicator vector $\boldsymbol{b}_n$, since there is no known relation between the wave locations of each beat, these sets of parameters $\boldsymbol{b}_n, \boldsymbol{b}_{n-1}, \boldsymbol{b}_{n-2}, \ldots$ are modeled as a priori mutually independent of each other. The indicators $b_{n,k}$ contained in $\boldsymbol{b}_n$ are subject to a *block constraint*: within $\mathcal{J}_{\mathrm{T},n}$, there is one T wave (such that $\|\boldsymbol{b}_n\| = 1$) or none (with $\|\boldsymbol{b}_n\| = 0$). Therefore, we define the prior of $\boldsymbol{b}_n$ as a discrete distribution on the set $\left\{\boldsymbol{\beta}_0, \ldots, \boldsymbol{\beta}_j, \ldots, \boldsymbol{\beta}_{N_{\mathrm{T},n}}\right\}$ where $\boldsymbol{\beta}_j$ is a $N_{\mathrm{T},n} \times 1$ vector whose j-th entry is 1 and all remaining entries are zero ($\boldsymbol{\beta}_0$ is an all zero vector which represents the case where

there is no T wave). The prior of $\boldsymbol{b}_n$ can then be defined as

$$\Pr\left(\boldsymbol{b}_n = \boldsymbol{\beta}_j\right) = \frac{1}{N_{\mathrm{T},n}+1}, \quad j \in \{1, \ldots, N_{\mathrm{T},n}\}. \tag{6}$$

Since the ECG waveforms are usually similar for two consecutive beats, we propose to assign a random walk prior to the T waveform coefficient vector $\boldsymbol{\alpha}$

$$\boldsymbol{\alpha}_n = \boldsymbol{\alpha}_{n-1} + \boldsymbol{v}_{n-1} \tag{7}$$

where $\boldsymbol{\alpha}_{n-1}$ denotes the T waveform estimates of the $(n-1)$th beat and $\boldsymbol{v}_{n-1}$ is an additive Gaussian white noise vector denoted as $\boldsymbol{v}_{n-1} \sim \mathcal{N}\left(\boldsymbol{0}, \sigma_\alpha^2 \boldsymbol{I}_G\right)$, where $\boldsymbol{I}_G$ is the $G \times G$ identity matrix. The variance σ_α^2 determines how fast the waveform coefficients are expected to change with time. Initialization is done by setting $\hat{\boldsymbol{h}}_0 = \boldsymbol{H}\hat{\boldsymbol{\alpha}}_0$ equal to a Hanning window (see details in Section 4).

The T wave delineation and waveform estimation problem consists of estimating recursively the wave location $\boldsymbol{b}_n$ and the waveform coefficients $\boldsymbol{\alpha}_n$ from the measurements $\boldsymbol{y}_n$ defined in (4).

3. A MARGINALIZED PARTICLE FILTER

Our goal is to estimate jointly the discrete-valued indicator vector $\boldsymbol{b}_n$ and the waveform vectors $\boldsymbol{\alpha}_n$ i.e., estimate the state vector $\boldsymbol{x}_n$. In a Bayesian framework, all inference is based on the posterior distribution of the unknown parameters given the set of available observations, expressed as $p\left(\boldsymbol{x}_{0:n}|\boldsymbol{y}_{1:n}\right)$ with $\boldsymbol{x}_{0:n} = (\boldsymbol{x}_0, \ldots, \boldsymbol{x}_n)$. PFs are a class of methods well-suited to perform the estimation of the hybrid state vector $\boldsymbol{x}_{0:n}$. They approximate the target distribution by an empirical distribution

$$\hat{p}\left(\boldsymbol{x}_{0:n}|\boldsymbol{y}_{1:n}\right) = \sum_{i=1}^{N_s} w_n^i \delta\left(\boldsymbol{x}_{0:n} - \boldsymbol{x}_{0:n}^i\right), \quad \sum_{i=1}^{N_s} w_n^i = 1 \tag{8}$$

where δ is the Dirac delta function. The weights w_n^i and the particles $\boldsymbol{x}_{0:n}^i$ are classically obtained by sequential importance sampling and a selection step to prevent degeneracy [8].

While the classical PFs are fairly easy to implement, a main drawback is that the required particle number increases quickly with the state dimension. The MPF can reduce the number of parameters estimated by the particle filtering and therefore allows one to use fewer particles. More specifically, when there is a linear Gaussian sub-structure in the state parameters $\boldsymbol{x}_n$, state estimates can be obtained by exploiting this structure. The key idea is to split $\boldsymbol{x}_n$ as follows

$$\boldsymbol{x}_n = \left[\left(\boldsymbol{x}_n^{\mathrm{L}}\right)^T, \left(\boldsymbol{x}_n^{\mathrm{NL}}\right)^T\right]^T \tag{9}$$

where $\boldsymbol{x}_n^{\mathrm{L}}$ denotes the state parameters with conditionally linear dynamic and $\boldsymbol{x}_n^{\mathrm{NL}}$ denotes the nonlinear state parameters. Using Bayes' theorem we can then marginalize out the linear state parameters and estimate them using the Kalman filter (KF), which is the optimal filter for this case. The nonlinear state variables are then estimated using a PF. Note that one KF is then associated with each particle.

It can be observed from (4) that both the discrete parameter vector $\boldsymbol{b}_n$ and the continuous parameter vector $\boldsymbol{\alpha}_n$ are conditionally linear sub-structures with respect to the observation $\boldsymbol{y}_n$. Since only the continuous parameters can be handled by the Kalman filtering, we choose $\boldsymbol{x}_n^{\mathrm{L}} = \boldsymbol{\alpha}_n$ and $\boldsymbol{x}_n^{\mathrm{NL}} = \boldsymbol{b}_n$. Thus $\boldsymbol{\alpha}_n$ can be handled by the Kalman filter. Analytically marginalizing out the linear state variables from $p\left(\boldsymbol{x}_{0:n}|\boldsymbol{y}_{1:n}\right)$ and using Bayes' theorem yields

$$p(\boldsymbol{b}_{0:n}, \boldsymbol{\alpha}_n|\boldsymbol{y}_{1:n}) = \underbrace{p(\boldsymbol{\alpha}_n|\boldsymbol{b}_{0:n}, \boldsymbol{y}_{1:n})}_{\text{Optimal KF}} \underbrace{p(\boldsymbol{b}_{0:n}|\boldsymbol{y}_{1:n})}_{\text{PF}} \tag{10}$$

The MPF recursions are summarized in Algorithm 1. The different steps involved in this algorithm are detailed in the rest of this section. Note that N_s is the number of particles.

Algorithm 1 Marginalized particle filter

{Initialization}
for particles $i = 1, \ldots, N_s$ **do**
  Set $\boldsymbol{b}_0^i = \boldsymbol{0}_{N_n \times 1}$, $\boldsymbol{\alpha}_0^i = \boldsymbol{H}^{-1}\hat{\boldsymbol{h}}_0$, $P_0^i = \boldsymbol{0}_{G\times G}$, $w_0^i = 1$.
end for
{Iterations}
for $n = 1, 2, \ldots,$ **do**
  for particles $i = 1, \ldots, N_s$ **do**
    {Kalman filter and Particle filter propagation}
    Kalman filter prediction for $\boldsymbol{\alpha}_n^i$ (see (11))
    Sample $\boldsymbol{b}_n^i \sim \Pr(\boldsymbol{b}_n = \boldsymbol{\beta}_j|\boldsymbol{b}_{0:n-1}^i, \boldsymbol{y}_{1:n})$ (see (12))
    Kalman filter correction for $\boldsymbol{\alpha}_n^i$ (see (13))
    Evaluate weights
    $$w_n^i = w_{n-1}^i \sum_{j \in \mathcal{J}_{\mathrm{T},n}} p(\boldsymbol{y}_n|\boldsymbol{b}_n^i = \boldsymbol{\beta}_j, \boldsymbol{y}_{1:n-1}) p(\boldsymbol{b}_n^i = \boldsymbol{\beta}_j)$$
  end for
  {Weight normalization}
  for particles $i = 1, \ldots, N_s$ **do**
    $w_n^i = w_n^i / \sum_{i=1}^{N_s} w_n^i$
  end for
  { State estimation}
  Estimation of $\boldsymbol{b}_n$ and $\boldsymbol{\alpha}_n$ (see (14))
  {Particle resampling}
  Calculate $\hat{N}_{\text{eff}} = 1/\sum_{i=1}^{N_s}\left(w_n^i\right)^2$
  if $\hat{N}_{\text{eff}} \leq 0.7N_s$ **then**
    Resample using systematic sampling scheme
  end if
end for

Kalman filter prediction. By using (7), the prediction step in the Kalman filter can be written as follows

$$\boldsymbol{\alpha}_{n|n-1}^i = \boldsymbol{\alpha}_{n-1}^i, \quad P_{n|n-1}^i = P_{n-1}^i + Q \tag{11}$$

where $\boldsymbol{\alpha}_{n|n-1}^i = \mathrm{E}\left[\boldsymbol{\alpha}_n|\boldsymbol{y}_{1:n-1}, \boldsymbol{b}_{0:n-1}^i\right]$, $Q = \sigma_\alpha^2 \boldsymbol{I}_{2L+1}$ and $P_{n|n-1}^i = \mathrm{Cov}\left[\boldsymbol{\alpha}_n|\boldsymbol{y}_{1:n-1}, \boldsymbol{b}_{0:n-1}^i\right]$. Note that the predicted state vector and its covariance computed by the KF are directly used to propagate the particles and compute their importance weights.

Proposal distribution for the indicators. It is well-known that the choice of the importance distribution is a critical issue to design efficient PF algorithms. To generate samples in interesting regions of the state space, i.e., corresponding to a high likelihood $p(\boldsymbol{y}_n|\boldsymbol{x}_n)$, a natural strategy consists of taking into account information from the most recent observations $\boldsymbol{y}_n$. The optimal importance distribution in the sense that it minimizes the variance of the importance weights is $q(\boldsymbol{x}_n|\boldsymbol{x}_{0:n-1}^i, \boldsymbol{y}_{0:n}) = p(\boldsymbol{x}_n|\boldsymbol{x}_{0:n-1}^i, \boldsymbol{y}_n)$ [14]. By inserting the Kalman filter prediction of (11), the optimal proposal distribution for $\boldsymbol{b}_{\mathrm{T},n}$ can be written as

$$\Pr(\boldsymbol{b}_n = \boldsymbol{\beta}_j|\boldsymbol{b}_{0:n-1}^i, \boldsymbol{y}_{1:n}) \propto \mathcal{N}\left(\tilde{\boldsymbol{y}}_{n,j}^i, \tilde{S}_{n,j}^i\right) \tag{12}$$

with

$$\tilde{\boldsymbol{y}}_{n,j}^i = \boldsymbol{B}_{n,j}\boldsymbol{H}\boldsymbol{\alpha}_{n|n-1}^i$$
$$\tilde{S}_{n,j}^i = \boldsymbol{B}_{n,j}P_{n|n-1}^i\boldsymbol{B}_{n,j}^T + R$$

where $\boldsymbol{B}_{n,j}$ is the $N_{\mathrm{T},n} \times (2L+1)$ Toeplitz matrix with first row $(b_{n,L+1} \cdots b_{n,1}\ 0 \cdots 0)$ and first column $(b_{n,L+1} \cdots b_{n,N_{\mathrm{T},n}}\ 0 \cdots 0)^T$ which corresponds to $\boldsymbol{b}_n = \boldsymbol{\beta}_j$, and $R = \sigma_w^2 \boldsymbol{I}_{N_{\mathrm{T},n}}$.

Kalman filter correction. After receiving the observation at time step n, the waveform coefficients can be updated for each generated wave indicator particle $\boldsymbol{b}_n^i$. The Kalman filter correction procedure can be written as

$$\begin{aligned} S_n^i &= \boldsymbol{B}_n^i P_{n|n-1}^i \left(\boldsymbol{B}_n^i\right)^T + R \\ K &= P_{n|n-1}^i \left(\boldsymbol{B}_n^i\right)^T \left(S_n^i\right)^{-1} \\ \boldsymbol{\alpha}_n^i &= \boldsymbol{\alpha}_{n|n-1}^i + \boldsymbol{H}^{-1} K(\boldsymbol{y}_n - \boldsymbol{B}_n^i \boldsymbol{H} \boldsymbol{\alpha}_{n|n-1}^i) \\ P_n^i &= (\boldsymbol{I} - K\boldsymbol{B}_n^i) P_{n|n-1}^i \end{aligned} \tag{13}$$

where $\boldsymbol{B}_n^i$ is the Toeplitz matrix $(N_{\mathrm{T},n}+L)\times(L+1)$ corresponding to the wave indicator particle vector $\boldsymbol{b}_n^i$.

State estimation. The sample-based blockwise MAP detector is used for estimating the binary sequence $\boldsymbol{b}_n$, while for the waveform coefficients $\boldsymbol{\alpha}_n$, a smooth state estimation is applied

$$\hat{\boldsymbol{b}}_n = \underset{\boldsymbol{b}_n^i \in \{0,1\}^{N_{\mathrm{T},n}}}{\operatorname{argmax}} \ \hat{p}(\boldsymbol{b}_n^i | \boldsymbol{y}_{1:n}, \boldsymbol{\alpha}_{0:n-1}), \quad \hat{\boldsymbol{\alpha}}_n = \sum_{i=1}^{N_s} \boldsymbol{\alpha}_n^i w_n^i. \tag{14}$$

The wave delineation consists of determining the peak and boundaries of the detected T and P waves. As mentioned previously, the wave indicator estimated by the MPF directly indicates the middle of the alloted waveform time window. Thus, the peak of the respective T or P wave can be obtained by shifting the indicator to the maximum position of the estimated waveform. Concerning the wave boundaries, since the estimated waveforms carry information about the wave morphology, they can be located by using the delineation criterion based on the waveform estimate as in [6, 7].

4. SIMULATION RESULTS

We evaluated the performance of the proposed algorithm on the QT database (QTDB) [11]. The QTDB contains 105 excerpts of Holter recordings from several widely used ECG databases, chosen to include a variety of P and T wave morphologies. The fixed hyperparameters involved in the prior distributions were chosen as $\sigma_\alpha^2 = 0.01$ and $\sigma_w^2 = 0.1$. These values allow for an appropriate waveform variability from one beat to another. Note that the non-QRS components are normalized by using the corresponding R peak values to handle different amplitude resolutions. The waveform vector $\hat{\boldsymbol{h}}_0 = \boldsymbol{H}\hat{\boldsymbol{\alpha}}_0$ was initialized with a $2L+1$ Hanning window whose amplitude was half the R peak. We have chosen $N_s = 200$ particles for all the following simulations.

Fig. 2 shows qualitative comparisons of the proposed MPF method with the Gaussian mixture model and extended Kalman filter (EKF) method of [4] and with the recently proposed multiple-beat Bayesian model and partially collapsed Gibbs sampler (PCGS) method of [6]. To evaluate the three methods under real physiological noise conditions, we have added electrode motion (EM) noise from the MIT-BIH noise stress test database. Fig. 2(a)(1) shows a segment of QTDB sele0136. Fig. 2(a)(2) shows the same segment corrupted by EM noise with a signal-to-noise ratio (SNR) of 10dB. The estimated non-QRS signal component obtained from the noisy signal by the three methods are depicted in Fig. 2(a)(3), Fig. 2(a)(4) and Fig. 2(a)(5). The original (noise-free) ECG signal is also shown

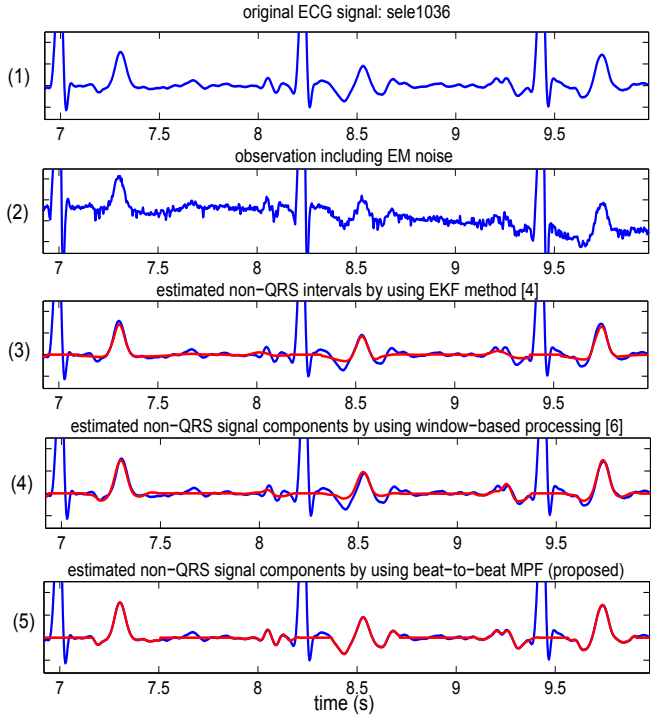

(a) QTDB-sele0136

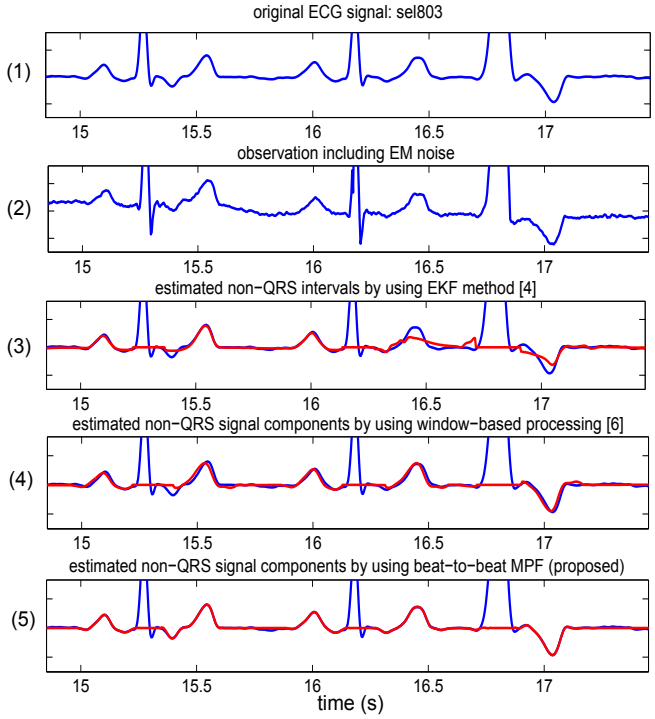

(b) QTDB-sel803

Fig. 2. Results of processing ECG datasets (a) "sele0136" and (b) "sel803". Captions for each subfigure: (1) Clean segment from QTDB; (2) noisy version including EM noise with SNR = 10dB; (3) non-QRS signal component estimated by the EKF method of [4] (red) and original signal (blue); (4) non-QRS signal component estimated by the window-based Bayesian method of [6] (red) and original signal (blue); (5) non-QRS signal component estimated by the proposed beat-to-beat MPF method (red) and original signal (blue).

for comparison. It can be seen that the proposed MPF method provides the closest agreement with the original ECG signal, especially at the onsets and ends of the waves, which is a desirable property for wave delineation. Fig. 2(b) shows analogous results for a segment of sel803 that contains premature ventricular contractions (a pathology which has parts of the T waves crossing the interval border and the P waves missing). For the proposed MPF method, this can be handled by including in the T wave interval observations $\boldsymbol{y}_{\mathrm{T}}$ the first L samples of the following P wave interval, where L is the half of the alloted waveform length. This allows a complete T waveform estimation in case the wave indicator locates at the last sample of $\mathcal{J}_{\mathrm{T}}$. Since one non-QRS interval is processed sequentially from a T wave interval to a P wave interval, the estimated T wave portion within the overlapped part can be extracted. Again, it can be seen that the estimates obtained with the proposed method are better than those obtained with the other two methods.

An important issue of PF methods is the number of particles. Table 1 shows the normalized mean square error (NMSE) of estimated non-QRS components versus the number of particles N_s. As can be seen, benefiting from the optimal importance distribution introduced in Section 3, good estimation performance can be obtained with a moderate number of particles. Note that for the proposed method using 200 particles, the processing time per beat is approximately 0.5s for a nonoptimized MATLAB implementation running on a 3.0-GHz Pentium IV computer, compared to about 2s for the method of [6].

For a quantitative analysis, Table 2 presents the means (μ) and standard deviations (σ) of the differences between the automated delineation results and the manual annotations, for the proposed algorithm and for two alternative methods: the PCGS method of [6] and the wavelet transform (WT) method of [3]. It is seen that the proposed algorithm outperforms the other methods in terms of both detection sensitivity[2] and delineation accuracy.

Table 1. Normalized mean square error (NMSE) versus number of particles

N_s	10	50	100	200	300
NMSE	-25dB	-31dB	-34dB	-40dB	-42dB

Table 2. Delineation and detection performance for QTDB

Parameter	Proposed alg.	PCGS [6]	WT [3]
$\boldsymbol{b}_{\mathrm{P}}$: Se (%)	99.45	98.93	98.87
Onset-P: $\mu \pm \sigma$ (ms)	3.1 ± 8.3	3.7 ± 17.3	2.0 ± 14.8
Peak-P: $\mu \pm \sigma$ (ms)	1.2 ± 5.3	4.1 ± 8.6	3.6 ± 13.2
End-P: $\mu \pm \sigma$ (ms)	2.7 ± 9.8	-3.1 ± 15.1	1.9 ± 12.8
$\boldsymbol{b}_{\mathrm{T}}$: Se (%)	100	99.81	99.77
Onset-T: $\mu \pm \sigma$ (ms)	6.5 ± 16.3	7.1 ± 18.5	N/A
Peak-T: $\mu \pm \sigma$ (ms)	-0.4 ± 4.8	1.3 ± 10.5	0.2 ± 13.9
End-T: $\mu \pm \sigma$ (ms)	-3.8 ± 14.2	4.3 ± 20.8	-1.6 ± 18.1

5. CONCLUSION

We introduced a sequential Bayesian method performing joint P and T wave delineation and waveform estimation on a beat-to-beat basis. Following the sequential Monte Carlo analysis principle, the sequential yet pseudo-cyclostationary nature of the ECG signal has been exploited by using a dynamic model under the Bayesian framework. A marginalized particle filter has been proposed to efficiently resolve the unknown parameters of the dynamic model. The proposed method was validated using the entire annotated QT database. This validation demonstrated reliable detection and accurate delineation for a wide variety of wave morphologies. A comparison with the window-based Gibbs sampling method of [6] and other state-of-the-art methods demonstrated significant improvements regarding T and P wave detection rate, positive predictivity, and delineation accuracy. Further advantage of this method includes the possibility of analyzing the beat-to-beat variation and evolution of the T and P waveforms. Thus it is ideally suited for real-time ECG monitoring and for on-line arrhythmia analysis. Future work includes the consideration of the local ECG baseline variations within each beat by using a polynomial model as in [7].

[2]The sensitivity (also referred to as detection rate) is defined as $\mathrm{Se} \triangleq N_{\mathrm{TP}}/(N_{\mathrm{TP}} + N_{\mathrm{FN}})$, where N_{TP} is the number of true positive detections and N_{FN} is the number of false negative detections [3].

6. REFERENCES

[1] N. V. Thakor and Y. S. Zhu, "Application of adaptive filtering to ECG analysis: Noise cancellation and arrhythmia detection," *IEEE Trans. Biomed. Eng.*, vol. 38, no. 8, pp. 785–793, 1991.

[2] P. Laguna, R. Jané, and P. Caminal, "Automatic detection of wave boundaries in multilead ECG signals: Validation with the CSE database," *Comput. Biomed. Res.*, vol. 27, no. 1, pp. 45–60, 1994.

[3] J. P. Martínez, R. Almeida, S. Olmos, A. P. Rocha, and P. Laguna, "A wavelet-based ECG delineator: Evaluation on standard databases," *IEEE Trans. Biomed. Eng.*, vol. 51, no. 4, pp. 570–581, 2004.

[4] O. Sayadi and M. B. Shamsollahi, "A model-based Bayesian framework for ECG beat segmentation," *J. Physiol. Meas.*, vol. 30, pp. 335–352, 2009.

[5] M. B. Conover, *Understanding Electrocardiography*. St. Louis: Mosby, 2003.

[6] C. Lin, C. Mailhes, and J.-Y. Tourneret, "P- and T-wave delineation in ECG signals using a Bayesian approach and a partially collapsed Gibbs sampler," *IEEE Trans. Biomed. Eng.*, vol. 57, no. 12, pp. 2840–2849, Dec. 2010.

[7] C. Lin, G. Kail, J.-Y. Tourneret, C. Mailhes, and F. Hlawatsch, "P and T wave delineation and waveform estimation in ECG signals using a block Gibbs sampler," in *Proc. IEEE ICASSP 2011*, Prague, Czech Republic, May 2011, pp. 537–540.

[8] A. Doucet, N. de Freitas, and N. Gordon, *Sequential Monte Carlo Methods in Practice*. New York, NY: Springer-Verlag, 2001.

[9] A. Doucet, N. Gordon, and V. Krishnamurthy, "Particle filters for state estimation of jump Markov linear systems," *IEEE Trans. Signal Process.*, vol. 49, no. 3, pp. 613–624, 2001.

[10] T. Schön, F. Gustafsson, and P.-J. Nordlund, "Marginalized particle filters for mixed linear/nonlinear state-space models," *IEEE Trans. Signal Process.*, vol. 53, no. 7, pp. 2279–2289, 2005.

[11] P. Laguna, R. Mark, A. Goldberger, and G. Moody, "A database for evaluation of algorithms for measurement of QT and other waveform intervals in the ECG," in *Proc. Comput. Cardiol.*, Lund, Sweden, Aug. 1997, pp. 673–676.

[12] J. Pan and W. J. Tompkins, "A real-time QRS detection algorithm," *IEEE Trans. Biomed. Eng.*, vol. 32, no. 3, pp. 230–236, 1985.

[13] V. S. Chouhan and S. S. Mehta, "Total removal of baseline drift from ECG signal," in *Proc. Int. Conf. Comput.: Theory Appl.*, Kolkata, India, March 2007, pp. 512–515.

[14] A. Doucet, S. Godsill, and C. Andrieu, "On sequential Monte Carlo sampling methods for Bayesian filtering," *Statistics and Computing*, vol. 10, pp. 197–208, 2000.